Role of d-wave pairing in A15 superconductors

S. Mukherjee and D. F. Agterberg

Phys. Rev. B **84**, 134520 — Published 17 October 2011

DOI: 10.1103/PhysRevB.84.134520

Role of d-wave pairing in $A15$ superconductors.

S. Mukherjee
NBIA, Niels Bohr Institute, Blegdamsvej 17, 2100 Copenhagen Ø, Denmark and
Department of Physics, University of Wisconsin-Milwaukee, Milwaukee, WI 53211

D. F. Agterberg
Department of Physics, University of Wisconsin-Milwaukee, Milwaukee, WI 53211

We argue that the recent Raman spectroscopy observation of a sharp mode in s-wave superconducting V_3Si is due to a competing d-wave pairing state. We present microscopic arguments for the origin of this d-wave order. We further argue that the d-wave order explains the observed shrinking of the vortex core structure at anomalously low magnetic fields and the large anisotropy observed in the upper critical field.

I. INTRODUCTION

Competing pairing channels have played a prominent role in theories of superfluid ^{3}He, cuprate, and pnictide superconductors. In p-wave ^{3}He, an excited pair state, stemming from a competing f-wave channel, has been observed through interferometry in an acoustic cavity[1]. The observation of this f-wave pairing channel leads to predictions of rich physics near impurities, surfaces, and vortices. In the cuprates, a competing s-wave or d_{xy} order has been invoked to interpret the properties of surface Andreev bound states[2]. More recently in the superconducting pnictides, many theories find that a sign changing s-wave state and a competing d-wave state have close transition temperatures[3], leading to the prediction of a pair collective mode observable through Raman spectroscopy and a superconducting state that breaks time reversal symmetry[4].

In this work we argue that $A15$ superconductors provide an ideal candidate for competing superconducting order. We show it is natural to expect an attractive d-wave pairing channel in addition to the attractive s-wave pairing channel in $A15$ materials. Specifically, the d-wave pairing belongs to the cubic E_g representation. This representation has two degenerate states with the same symmetry properties as $k_x^2 - k_y^2$ and $(2k_z^2 - k_x^2 - k_y^2)/\sqrt{3}$. The primary experimental motivation for exploring this state is Raman spectroscopy. Raman active superconducting gap modes have been seen in Nb_3Sn and in V_3Si[5]. Modes have been found in three symmetries: A_{1g}, E_g, and F_{2g}. The modes in the E_g channel are significantly sharper and occur at lower energies than those in the A_{1g} and F_{2g} channels. We argue that the E_g modes are due to an attractive d-wave pairing channel that arises from the unique structure of cubic $A15$ materials. This d-wave order does not play an important role in the ground state thermodynamics but, as we show below, it is important for understanding the superconducting state of A15 materials in magnetic fields.

Many $A15$s are type II superconductors with transition temperature (T_c) on the order of 20 K[6]. Their cubic structure (space group $Pm3n$) contains the formulae unit A_3B. The B atoms form a cubic lattice while the A atoms form three sets of orthogonal chains that run through the faces of the cube[7]. These chains play an important role in understanding these materials. For example, interactions on these chains drive the Martensitic cubic to tetragonal transition that appears in some of these materials[8,9]. Early theories assumed the electronic states on the chains to be one-dimensional[10,11]. However, it was later found that this was an oversimplification[12,13]. Nevertheless, the band structure shows strong anisotropies that originate from electrons residing on the chains[21]. In accord with this, we assume that the superconducting condensation energy is dominated by electrons on the three orthogonal chains. This naturally leads to *three* order parameters $\Psi = (\psi_x, \psi_y, \psi_z)$ corresponding to superconductivity on each of the three chains (we call this the chain basis). In the following we exploit this chain basis to show how a d-wave collective mode arises that can account for the Raman spectroscopy data. We then turn to the development of a microscopic model that provides an estimate for the pairing interactions in the s and d-wave channels. Finally, we consider the appearance of the d-wave order when magnetic fields are applied.

II. GROUND STATE AND d-WAVE COLLECTIVE MODE

To address the origin of collective modes, we begin with a Ginzburg Landau (GL) theory that is based solely on symmetry arguments. We use the chain basis to write this theory, in which case the GL free energy density is

$$f = \alpha \sum_i |\psi_i|^2 + \epsilon \sum_{i\neq j} \psi_i \psi_j^* + \kappa_1 \sum_i |D_i \psi_i|^2 + \kappa_2 \sum_{i\neq j} |D_i \psi_j|^2 + \kappa_3 \sum_{l,i\neq j} (D_l \psi_i)(D_l \psi_j)^* + \kappa_4 \sum_{l\neq i\neq j} (D_l \psi_i)(D_l \psi_j)^*$$

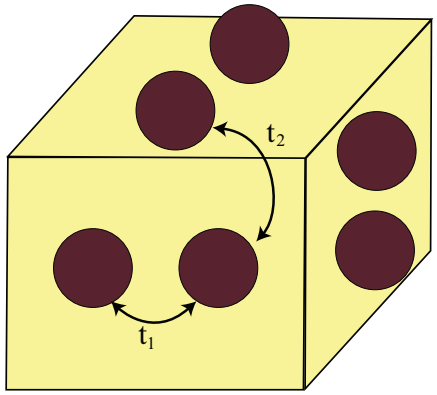

FIG. 1. Position of Vanadium atoms in the unit cell and the corresponding hopping matrix elements included in the Hamiltonian.

$$+ \beta_1 \sum_i |\psi_i|^4 + \sum_{i\neq j} (\beta_2 \psi_i^2 \psi_j^{*2} + \beta_3 |\psi_i|^2 |\psi_j|^2) + \sum_{l\neq i\neq j} (\beta_4 \psi_i \psi_j^* |\psi_l|^2 + \beta_5 (\psi_i \psi_j \psi_l^{*2} + c.c)$$
$$+ \beta_6 \sum_{l\neq i\neq j} ((\psi_i + \psi_j)\psi_l^* + c.c)|\psi_l|^2) \quad (1)$$

where $D_i = -i\partial_i - 2eA_i/c$, $\mathbf{A}$ is the vector potential, and *c.c.* represents complex conjugate. Depending upon the coefficients ϵ and β_i, Eq. 1 allow for four possible ground states: $\Psi_s \propto (1,1,1)$, $\Psi_d \propto (1, e^{i2\pi/3}, e^{i4\pi/3})$, $\Psi_{d,1} \propto (1,-1,0)$, or $\Psi_{d,2} \propto (-1,-1,2)$. The state Ψ_s has s-wave symmetry (A_{1g}) while the states $\Psi_d, \Psi_{d,1}, \Psi_{d,2}$ all are d-wave, belonging to the E_g representation. The state Ψ_s will be stable if $\epsilon < 0$ while one of the states Ψ_d, Ψ_{d1}, or Ψ_{d2} will be stable if $\epsilon > 0$. Physically, it is expected that gap on each chain is maximized to maximize the condensation energy. This implies that the states $\Psi_{d,1}$ and $\Psi_{d,2}$ are unlikely to be realized. Of the remaining two states, the most likely is Ψ_s as the preponderance of evidence suggests an s-wave ground state in $A15$ superconductors. In the following it is assumed that Ψ_s is the ground state. However, it should be noted that it is possible that Ψ_d is the ground state of some $A15$ superconductors.

We now turn to possible collective modes of Ψ_s. Since our order parameter has six complex degrees of freedom, there can exist six collective modes: the amplitude and phase modes for each of the chain gaps. The amplitude modes are likely to be strongly damped since the mode gaps will typically lie near the chain gap values. Furthermore, the phase mode in which all three chain order parameters oscillate in phase will be pushed to the Plasma frequency. This leaves two phase modes as candidates for collective modes. These modes correspond to relative phase oscillations between the chain order parameters and resemble Leggett modes of multiband superconductors[15]. To examine these two phase modes in more detail, we follow an approach developed in Ref. 16 in the context of unconventional superconductors. We represent the order parameter as $\Psi = \psi_0(e^{i\theta_1}, e^{i\theta_2}, e^{i\theta_3})/\sqrt{3}$. We use the Josephson relation $\hbar\partial\theta_\alpha/\partial t = -\mu_\alpha$ together with the quasi-conservation laws $\hbar\partial\mu_\alpha/\partial t = (\partial\mu_\alpha/\partial N_\alpha)(\partial F/\partial\theta_\alpha)$ where μ_α is the chemical potential, F is the free energy, and N_α the particle number corresponding to quasi-particles on chain α. This yields a two-fold degenerate relative phase mode with d-wave E_g symmetry that has a frequency given by

$$\omega_0^2 = \frac{2}{3\hbar^2 N(0)} \left[3|\epsilon|\psi_0^2 - (4\beta_2 + \beta_4 + 3\beta_5 + 2\beta_6)\psi_0^4\right] \quad (2)$$

where $N(0) \equiv \partial N_\alpha/\partial\mu_\alpha$, is the density of states for each of the chains.

In the limit $\epsilon = \beta_2 = \beta_4 = \beta_5 = \beta_6 = 0$, this gives $\omega_0 = 0$. In this limit, the chains are uncoupled and the theory has an accidental $U(1)\times U(1)\times U(1)$ symmetry associated with the independent variations of the phase of each chain. The microscopic theory presented later reveals that $4\beta_2 + \beta_4 + 3\beta_5 + 2\beta_6 < 0$, so that ω_0 is well defined. If $\omega_0 < 2\Delta_0$, where Δ_0 is the chain gap value, these modes will be weakly damped and provide a natural explanation for the Raman spectroscopy results of Ref. 5.

III. MICROSCOPIC THEORY

Now we turn to a microscopic model to examine how an attractive d-wave pairing channel can appear in A15 materials and also to determine the phenomenological coefficients in the GL theory. LDA calculations show that near the Fermi energy, the $3z^2 - r^2$ orbitals on the A atoms that form chains along the z-direction and symmetry equivalent orbitals for the other two chains directions are the most important[17]. We therefore use a tight binding Hamiltonian

that includes a nearest neighbor (nn) intrachain hopping (t_1) as well as a next nearest neighbor (nnn) interchain hopping (t_2) between these orbitals (as shown in Fig. 1). This is similar to the approach used earlier by Bhatt[18]. To identify the interactions that lead to superconductivity, we note that there is compelling evidence for strong electron phonon (ep) coupling in $A15$ materials. In particular, phonon anomalies due to strong ep coupling of the chain atom displacements to electrons have been observed[19] that are in agreement with predictions from LDA calculations[17]. Additionally, tunneling data on superconducting Nb_3Sn reveal features of the phonon spectrum[20], showing that this coupling is responsible for superconductivity. The phonons that couple most strongly to electrons are intra-chain phonons[19]. We therefore use the following BCS Hamiltonian as a minimal model for $A15$ superconductors

$$H = t_1 \sum_{i\sigma<\nu\nu'>_{nn}} c^\dagger_{\nu i\sigma} c_{\nu' i\sigma} + t_2 \sum_{ij\sigma<\nu\nu'>_{nnn}} c^\dagger_{\nu i\sigma} c_{\nu' j\sigma} - V_0 \sum_i c^\dagger_{\nu i\uparrow} c^\dagger_{\nu i\downarrow} c_{\nu i\downarrow} c_{\nu i\uparrow} \tag{3}$$

where $c_{\nu j\sigma}$ destroys an electron with spin σ, with the Wannier function centered on the ν^{th} Vanadium atom in the j^{th} unit cell. The six Vanadium atoms in a unit cell along the x, y, and z chain directions have positions $\boldsymbol{r}_\nu = (\hat{\boldsymbol{y}}/2 \pm \hat{\boldsymbol{x}}/4, \hat{\boldsymbol{z}}/2 \pm \hat{\boldsymbol{y}}/4, \hat{\boldsymbol{z}}/2 \pm \hat{\boldsymbol{y}}/4)$ in units of lattice spacing with respect to the center of the unit cell. These three different chain directions also correspond to orbitals with symmetries $(3x^2 - r^2, 3y^2 - r^2, 3z^2 - r^2)$ centered on the Vanadium atoms respectively. Below we discuss in detail the tight binding Hamiltonian and the superconducting instability.

A. Tight Binding Hamiltonian

We diagonalize the above tight binding Hamiltonian by going to the Fourier space. For the annihilation operator this gives, $c_{\nu j\sigma} = \frac{1}{\sqrt{N}} \sum_{\boldsymbol{k}} e^{-i\boldsymbol{k}\cdot(\boldsymbol{r}_\nu + \boldsymbol{r}_j)} c_{\nu\sigma}(\boldsymbol{k})$ where $c_{\nu\sigma}(\boldsymbol{k})$ annihilates an electron on the ν^{th} Vanadium atom and has momentum $\boldsymbol{k}$. Similarly transforming the creation operators as well to the reciprocal space we can derive a tight binding Hamiltonian in reciprocal space which may be expressed in matrix form $H_0 = \sum_{\boldsymbol{k}} {\Psi_{\boldsymbol{k}}}^\dagger M_k \Psi_{\boldsymbol{k}}$, where for simplicity the spin indices have been suppressed. The matrix M_k is given by,

$$M_k = \begin{pmatrix} -\mu & \epsilon_x(\boldsymbol{k}) & \epsilon_{13}(\boldsymbol{k}) & \epsilon_{14}(\boldsymbol{k}) & \epsilon_{15}(\boldsymbol{k}) & \epsilon_{16}(\boldsymbol{k}) \\ \epsilon_x(\boldsymbol{k}) & -\mu & \epsilon_{23}(\boldsymbol{k}) & \epsilon_{24}(\boldsymbol{k}) & \epsilon_{25}(\boldsymbol{k}) & \epsilon_{26}(\boldsymbol{k}) \\ \epsilon^*_{13}(\boldsymbol{k}) & \epsilon^*_{23}(\boldsymbol{k}) & -\mu & \epsilon_z(\boldsymbol{k}) & \epsilon_{35}(\boldsymbol{k}) & \epsilon_{36}(\boldsymbol{k}) \\ \epsilon^*_{14}(\boldsymbol{k}) & \epsilon^*_{24}(\boldsymbol{k}) & \epsilon_z(\boldsymbol{k}) & -\mu & \epsilon_{45}(\boldsymbol{k}) & \epsilon_{46}(\boldsymbol{k}) \\ \epsilon^*_{15}(\boldsymbol{k}) & \epsilon^*_{25}(\boldsymbol{k}) & \epsilon^*_{35}(\boldsymbol{k}) & \epsilon^*_{45}(\boldsymbol{k}) & -\mu & \epsilon_y(\boldsymbol{k}) \\ \epsilon^*_{16}(\boldsymbol{k}) & \epsilon^*_{26}(\boldsymbol{k}) & \epsilon^*_{36}(\boldsymbol{k}) & \epsilon^*_{46}(\boldsymbol{k}) & \epsilon_y(\boldsymbol{k}) & -\mu \end{pmatrix} \tag{4}$$

and $\Psi_{\boldsymbol{k}} = (c_1(\boldsymbol{k}), c_2(\boldsymbol{k}), c_3(\boldsymbol{k}), c_4(\boldsymbol{k}), c_5(\boldsymbol{k}), c_6(\boldsymbol{k}))$. In the above 6×6 matrix, μ is the chemical potential that is adjusted to yield the correct qualitative form for the known Fermi surface sheets as evaluated from the full DFT calculations[21]. Here the terms $\epsilon_\alpha(\boldsymbol{k}) = 2t_1 \cos(k_\alpha/2)$ where $\alpha = \{x, y, z\}$ and the interchain terms are given by

$$\begin{aligned}
\epsilon_{24}(\boldsymbol{k}) &= 2t_2 e^{-i(k_x/4)} e^{-i(k_z/4)} \cos(k_y/2) \\
\epsilon_{23}(\boldsymbol{k}) &= 2t_2 e^{-i(k_x/4)} e^{i(k_z/4)} \cos(k_y/2) \\
\epsilon_{14}(\boldsymbol{k}) &= 2t_2 e^{i(k_x/4)} e^{-i(k_z/4)} \cos(k_y/2) \\
\epsilon_{13}(\boldsymbol{k}) &= 2t_2 e^{i(k_x/4)} e^{i(k_z/4)} \cos(k_y/2) \\
\epsilon_{26}(\boldsymbol{k}) &= 2t_2 e^{-i(k_x/4)} e^{-i(k_y/4)} \cos(k_z/2) \\
\epsilon_{25}(\boldsymbol{k}) &= 2t_2 e^{-i(k_x/4)} e^{i(k_y/4)} \cos(k_z/2) \\
\epsilon_{16}(\boldsymbol{k}) &= 2t_2 e^{i(k_x/4)} e^{-i(k_y/4)} \cos(k_z/2) \\
\epsilon_{15}(\boldsymbol{k}) &= 2t_2 e^{i(k_x/4)} e^{i(k_y/4)} \cos(k_z/2) \\
\epsilon_{46}(\boldsymbol{k}) &= 2t_2 e^{-i(k_z/4)} e^{-i(k_y/4)} \cos(k_x/2) \\
\epsilon_{45}(\boldsymbol{k}) &= 2t_2 e^{-i(k_z/4)} e^{i(k_y/4)} \cos(k_x/2) \\
\epsilon_{36}(\boldsymbol{k}) &= 2t_2 e^{i(k_z/4)} e^{-i(k_y/4)} \cos(k_x/2) \\
\epsilon_{35}(\boldsymbol{k}) &= 2t_2 e^{i(k_z/4)} e^{i(k_y/4)} \cos(k_x/2).
\end{aligned} \tag{5}$$

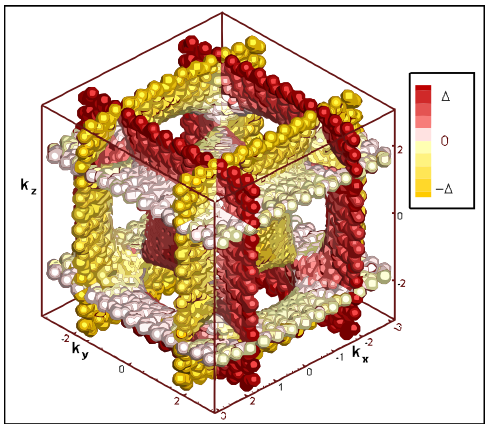

FIG. 2. The self-consistent $d_{x^2-y^2}$ like solution for the E_g symmetry gap function shown on the Fermi surface (for $t_2/t_1 = 0.22$). The gap values are represented by the different colors show in the box on the right. The (k_x, k_y, k_z) are in units of the inverse lattice spacing.

B. Superconductivity

As shown in Eq. 3, in addition to the tight binding Hamiltonian above, a superconducting instability is present in the system through the following quartic interaction term,

$$H_{BCS} = -V_0 \sum_{i\nu} c^\dagger_{\nu i\uparrow} c^\dagger_{\nu i\downarrow} c_{\nu i\downarrow} c_{\nu i\uparrow}, \tag{6}$$

The pairing interaction $-V_0 < 0$ corresponds to an effective interaction that would arise from ep coupling on the chains alone. The ep coupling gives rise to a local interaction that is retarded in time by an amount $\Delta t \sim 1/\omega_d$, where ω_d refers to the Debye frequency. This retardation is captured within BCS theory by restricting the energies of the electrons to lie within a cutoff ω_d of the Fermi energy.

To proceed, we diagonalize the tight binding Hamiltonian and this leads to six bands which typically leads to three Fermi surface sheets and a momentum dependent pairing interaction $V_{\alpha,\beta}(\boldsymbol{k}, \boldsymbol{k}')$. This gives a Hamiltonian given by,

$$H = \sum_{\alpha\sigma\boldsymbol{k}} \epsilon_\alpha(\boldsymbol{k}) a^\dagger_{\alpha\sigma}(\boldsymbol{k}) a_{\alpha\sigma}(\boldsymbol{k}) + \sum_{\alpha,\beta,\boldsymbol{k},\boldsymbol{k}',\boldsymbol{q}} V_{\alpha,\beta}(\boldsymbol{k}, \boldsymbol{k}') a^\dagger_{\alpha\uparrow}(\boldsymbol{k} + \boldsymbol{q}/2) a^\dagger_{\alpha\downarrow}(-\boldsymbol{k} + \boldsymbol{q}/2) a_{\beta\downarrow}(-\boldsymbol{k}' + \boldsymbol{q}/2) a_{\beta\uparrow}(\boldsymbol{k}' + \boldsymbol{q}/2) \tag{7}$$

where indices α, β that run from 1 to 6 represent the eigenstates of the diagonalized band Hamiltonian. If $\hat{c} = \hat{P}^\dagger \hat{a}$, where $\hat{U} = \hat{P}^\dagger$ is the transpose of the unitary eigenvector matrix whose components are U_{ij} then the momentum dependance of the quartic interaction term is

$$V_{\alpha,\beta}(\boldsymbol{k}, \boldsymbol{k}') = -V_0 \sum_i U^*_{i,\alpha}(\boldsymbol{k}) U^*_{i,\alpha}(-\boldsymbol{k}) U_{i,\beta}(-\boldsymbol{k}') U_{i,\beta}(\boldsymbol{k}'). \tag{8}$$

Treating this interaction within a mean-field theory and defining a $\boldsymbol{k}$-dependent gap on each of sheets of the Fermi surface, we get the following linearized gap equation

$$\Delta_\alpha(\boldsymbol{k}) = \ln\left(\frac{1.13\epsilon_D}{k_B T_c}\right) \sum_\beta \langle V_{\alpha,\beta}(\boldsymbol{k}, \boldsymbol{k}') \Delta_\beta(\boldsymbol{k}') N_\beta(\boldsymbol{k}') \rangle_{F.S} \tag{9}$$

where α, β correspond to the different bands, $\epsilon_\beta(\boldsymbol{k}')$ is the band energy, $\epsilon_D = \hbar\omega_D$, $N_\beta(\boldsymbol{k}') = 1/|\nabla_{\boldsymbol{k}'}[\epsilon_\beta(\boldsymbol{k}')]|$ is the density of states evaluated at the Fermi energy in the gap equation and the angular bracket implies average over the Fermi surface. To solve this equation we do not assume a $\boldsymbol{k}$-dependence for the gap but rather discretise the Fermi surface and explicitly find the eigenfunctions that solve this gap equation. We find that there are only two solutions, an s-wave A_{1g} solution and a d-wave E_g solution. It is possible to include Coulomb interactions analytically in the limit $t_2/t_1 = 0$ by using an Anderson-Morel type theory[22]. In this limit, we find that on-site Coulomb interactions have the same effect on both the s and d-wave solutions.

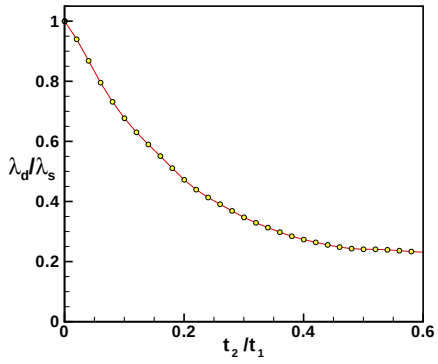

FIG. 3. Ratio of eigenvalues λ_d/λ_s vs t_2/t_1.

In Fig. 2, we show the self-consistent solution for the E_g gap degree of freedom corresponding to a $d_{x^2-y^2}$ symmetry. This solution is qualitatively different than the $k_x^2 - k_y^2$ solution expected for a spherical Fermi surface. In fact, it is more appropriately described as having three nearly constant gap amplitudes (denoted by $\Delta, 0, -\Delta$) which can be interpreted as the three chain gap values. In Fig. 3, we show the effective interactions for the A_{1g} and E_g pairing channels as a function of t_2/t_1 while keeping the Fermi surface volume constant (in the weak-coupling limit $T_c = \omega_D \exp\left(\frac{-1}{\lambda}\right)$ where λ is the effective interaction found from solving the gap equation).

IV. DERIVATION OF GL FREE ENERGY

We can derive the Ginzburg Landau free energy from the microscopic theory by including the spatial inhomogeneities in the gap function. The gap function is $\Delta_{\alpha,\uparrow\downarrow}(\boldsymbol{k},\boldsymbol{q}) = \sum_{\boldsymbol{k}',\beta} V_{\alpha,\beta}(\boldsymbol{k},\boldsymbol{k}')\langle a_{\beta,\uparrow}(\boldsymbol{k}+\boldsymbol{q}/2)a_{\beta,\downarrow}(-\boldsymbol{k}+\boldsymbol{q}/2)\rangle$ where α,β represent band indices and inhomogeneity of the order parameter is included through the center of mass momentum index $\boldsymbol{q}$ (this will allow the GL coefficients κ_i to be determined). The superconducting gap equation becomes

$$\Delta_\alpha(\boldsymbol{k},\boldsymbol{q}) = T\sum_{n,\beta,\boldsymbol{k}'} \frac{V_{\alpha,\beta}(\boldsymbol{k},\boldsymbol{k}')\Delta_\beta(\boldsymbol{k}',\boldsymbol{q})}{(\tilde{\omega}_n^2 + \epsilon_\beta^2(\boldsymbol{k}') + |\Delta_\beta(\boldsymbol{k}')|^2)} \tag{10}$$

where $\tilde{\omega}_n = (2n+1)\pi T + i\boldsymbol{q}\cdot\nabla_{\boldsymbol{k}'}\epsilon_\beta(\boldsymbol{k}')$.

Within a weak coupling approximation the gap equation close to the superconducting T_c can be integrated to yield the Ginzburg Landau free energy. The general method for performing this operation is well known[23]. Here we assign the order parameters ψ_s to the A_{1g} representation solution and (η_1,η_2) to the E_g representation of cubic symmetry. The superconducting gap can be expressed in terms of these order parameters in the form,

$$\Delta(\boldsymbol{k}) = \psi f_\psi(\boldsymbol{k}) + \eta_1 f_{\eta_1}(\boldsymbol{k}) + \eta_2 f_{\eta_2}(\boldsymbol{k}) \tag{11}$$

Here f_ψ is the s-wave basis function and $(f_{\eta_1},\ f_{\eta_2})$ correspond to the basis functions for the two dimensional E_g irreducible representation of cubic symmetry. Expanding the gap equation to second order in $\boldsymbol{q}$ and third order in the order parameter yields an equation that can be integrated in terms of the order parameter to obtain the Ginzburg Landau free energy.

Therefore using the above procedure and expanding the superconducting gap equation in the weak coupling limit close to the superconducting transition temperature the free energy in the s-d basis is obtained,

$$\begin{aligned}
&F = \alpha_s|\psi|^2 + \alpha_d|\boldsymbol{\eta}|^2 + \kappa_1'|\boldsymbol{D}\psi|^2 + \kappa_2'(|\boldsymbol{D}\eta_1|^2 + |\boldsymbol{D}\eta_1|^2) + \kappa_3'[(2(D_z\eta_2)(D_z\eta_2)^* - (D_x\eta_2)(D_x\eta_2)^* - (D_y\eta_2)(D_y\eta_2)^*)\\
&-(2(D_z\eta_1)(D_z\eta_1)^* - (D_x\eta_1)(D_x\eta_1)^* - (D_y\eta_1)(D_y\eta_1)^*) + \sqrt{3}((D_x\eta_1)(D_x\eta_2)^* - (D_y\eta_1)(D_y\eta_2)^* + c.c)]\\
&+\kappa_4'[\frac{1}{\sqrt{3}}(2(D_z\psi)(D_z\eta_2)^* - (D_x\psi)(D_x\eta_2)^* - (D_y\psi)(D_y\eta_2)^*) + ((D_x\psi)(D_x\eta_1)^* - (D_y\psi)(D_y\eta_1)^*) + c.c]\\
&+\beta_1'|\psi|^4 + \beta_2'|\boldsymbol{\eta}|^4 + \beta_3'|\boldsymbol{\eta}\cdot\boldsymbol{\eta}|^2 + \beta_4'|\psi|^2(|\eta_1|^2 + |\eta_2|^2) + \beta_5'[{\psi^*}^2(\eta_1^2 + \eta_2^2) + c.c]\\
&+\beta_6'[\psi^*(\eta_1|\eta_1|^2 - 2\eta_1|\eta_2|^2 - \eta_1^*\eta_2^2) + c.c]
\end{aligned} \tag{12}$$

Note that this is the most general free energy for the given representation allowed by cubic symmetry up to the fourth order in the expansion parameters. The weak coupling fourth order coefficients are numerically evaluated from the following Fermi surface averages

$$\begin{aligned}
\beta_1' &= \frac{c}{2}\langle f_\psi^4\rangle_{FS} \\
\beta_2' &= c\langle f_{\eta_1}^2 f_\psi^2\rangle_{FS} \\
\beta_3' &= \frac{c}{2}\langle f_{\eta_1}^2 f_{\eta_2}^2\rangle_{FS} \\
\beta_4' &= 2c\langle f_{\eta_1}^2 f_\psi^2\rangle_{FS} \\
\beta_5' &= \frac{c}{2}\langle f_{\eta_1}^2 f_\psi^2\rangle_{FS} \\
\beta_6' &= c\langle f_{\eta_1}^3 f_\psi\rangle_{FS}
\end{aligned} \tag{13}$$

here the constant $c = 7V_0\zeta(3)/(8\pi^2 T_c^2)$. Similarly the gradient term coefficients are given by

$$\kappa_1' = c/3\langle f_\psi^2 \boldsymbol{v}_F^2\rangle_{FS} \tag{14}$$
$$\kappa_2' = c/3\langle f_{\eta_1}^2 \boldsymbol{v}_F^2\rangle_{FS} \tag{15}$$
$$\kappa_3' = c/\sqrt{3}\langle f_{\eta_1} f_{\eta_2} v_{Fx}^2\rangle_{FS} \tag{16}$$
$$\kappa_4' = c\langle f_\psi f_{\eta_1} v_{Fx}^2\rangle_{FS} \tag{17}$$
$$\tag{18}$$

Here $\boldsymbol{v}_F$ is the Fermi velocity. Note that the basis functions $f(\boldsymbol{k})$ are the self consistent numerical solutions of the linear gap equation and no prior form has been assumed for them.

The corresponding free energy in the chain basis has been given in Eq. 1. The chain basis is formally given by $\psi_x = \psi_s/\sqrt{3} - \eta_1/\sqrt{6} + \eta_2/\sqrt{2}$, $\psi_y = \psi_s/\sqrt{3} - \eta_1/\sqrt{6} - \eta_2/\sqrt{2}$ and $\psi_z = \psi_s/\sqrt{3} - \eta_1\sqrt{\frac{2}{3}}$. The free energy in the chain basis follows from Eq. 12 by the following relations: $\beta_1' = \beta_2' = (\beta_1 + \beta_3)/3$, $\beta_3' = \beta_5'/2 = \beta_6'/(2\sqrt{2}) = (2\beta_1 - \beta_3)/12$, $\beta_4' = (4\beta_1 + \beta_3)/3$, $\kappa_1' = \kappa_2' = (3\kappa_1 + 2\kappa_2)/5$, $\kappa_3' = -\sqrt{3/8}\kappa_4' = -(3/10)(\kappa_1 - \kappa_2)$. The variation of the GL coefficient with the interchain chain hopping is shown in Fig. 4. Note that the largest coefficients are β_1, β_3, κ_1, and κ_2 and it would be reasonable to simplify the theory including only these terms in a GL analysis (as we have done). A similar simplification does not occur in the *s*-*d* basis.

V. MAGNETIC FIELDS

*A*15 superconductors exhibit anomalous properties in magnetic fields. Notably, these cubic materials have a large anisotropy in the upper critical field (H_{c2})[24] and they also exhibit a hexagonal to square vortex lattice transition at anomalously low magnetic fields[25]. This vortex transition is also accompanied by a sharp reduction in the coherence length[26,27]. Here we examine whether the appearance of *d*-wave order can provide an explanation for these observations.

A. Upper Critical Field

First we begin with the anisotropy in the upper critical field. In particular, H_{c2} in V_3Si shows an anisotropy that is estimated to be 20 % at the zero temperature[24]. H_{c2} is highest for the field along the $\langle 100\rangle$ direction, lower for fields along the $\langle 110\rangle$ direction, and lowest for the field along the $\langle 111\rangle$ direction[24]. We show in the following discussion that the GL theory of Eq. 1 above predicts that the same anisotropy in H_{c2} as observed experimentally (as described in the previous sentence). To show this the upper critical field may be evaluated by expressing the free energy in terms of the creation and annihilation operators which operate on the Landau levels. For a magnetic field along the z direction they are defined as,

$$\Pi_+ = \frac{l}{\sqrt{2}}(D_x + iD_y) \tag{19}$$

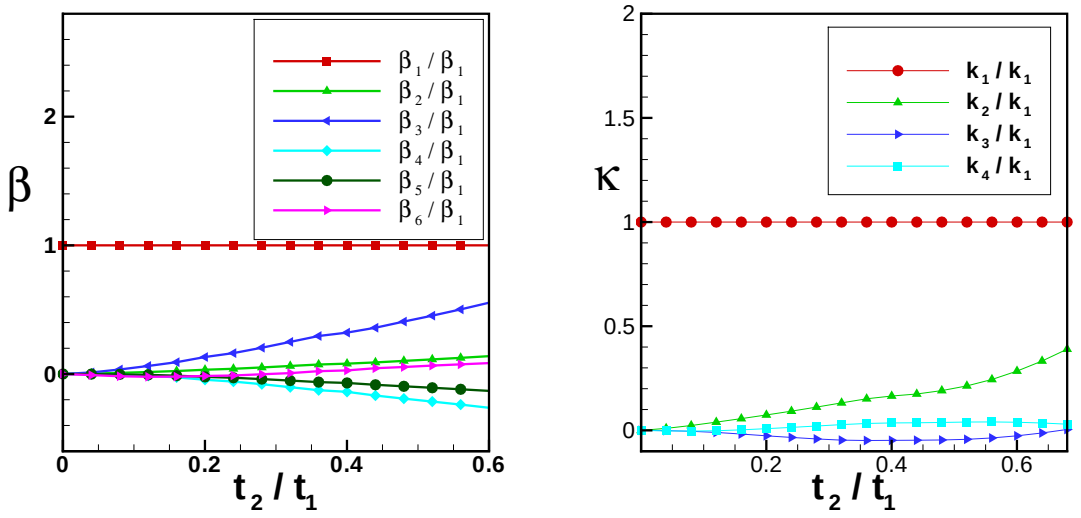

FIG. 4. Coefficients of the GL theory vs interchain interaction. The volume enclosed by the Fermi surface has been kept constant with the variation in t_2/t_1.

$$\Pi_- = \frac{l}{\sqrt{2}}(D_x - iD_y) \tag{20}$$

$$l^2 = \frac{\hbar c}{2eH} \tag{21}$$

with H being an external magnetic field applied along the z direction, and $D_\alpha = -i\partial_\alpha - 2eA_\alpha/c$. Expressing the equivalent operators for the different directions of magnetic field we can then write the quadratic portion of the free energy for the magnetic field along the $(1,0,0)$ and $(1,1,0)$ direction in the matrix form as,

$$f_{100} = \begin{pmatrix} \psi^* & \eta_1^* & \eta_2^* \end{pmatrix} \begin{pmatrix} \kappa_1\Pi_0 + \alpha_s & \frac{\kappa_4}{\sqrt{3}}\Pi_2 & -\kappa_4\Pi_1 \\ \frac{\kappa_4}{\sqrt{3}}\Pi_2 & \kappa_2\Pi_0 - \kappa_3\Pi_2 + \alpha_d & -\sqrt{3}\kappa_3\Pi_1 \\ -\kappa_4\Pi_1 & -\sqrt{3}\kappa_3\Pi_1 & \kappa_2\Pi_0 + \kappa_3\Pi_2 + \alpha_d \end{pmatrix} \begin{pmatrix} \psi \\ \eta_1 \\ \eta_2 \end{pmatrix} \tag{22}$$

$$f_{110} = \begin{pmatrix} \psi^* & \eta_1^* & \eta_2^* \end{pmatrix} \begin{pmatrix} \kappa_1\Pi_0 + \alpha_s & \frac{\kappa_4}{\sqrt{3}}\Pi_2 & 0 \\ \frac{\kappa_4}{\sqrt{3}}\Pi_2 & \kappa_2\Pi_0 - \kappa_3\Pi_2 + \alpha_d & 0 \\ 0 & 0 & \kappa_2\Pi_0 + \kappa_3\Pi_2 + \alpha_d \end{pmatrix} \begin{pmatrix} \psi \\ \eta_1 \\ \eta_2 \end{pmatrix} \tag{23}$$

Here $\Pi_0 = 1/l^2(1 + 2\Pi_+\Pi_-)$, $\Pi_1 = 1/(2l^2)(\Pi_0 + \Pi_+^2 + \Pi_-^2)$, $\Pi_2 = 1/(2l^2)(\Pi_0 - 3(\Pi_+^2 + \Pi_-^2))$. Note that the (1,1,0) free energy has been written in the rotated basis with $x' = z$, $y' = (x-y)/\sqrt{2}$, and $z' = (x+y)/\sqrt{2}$.

Comparing the upper critical field along the $(1,0,0)$ and $(1,1,0)$ magnetic field directions, we find that the free energy for the $(1,0,0)$ direction contains additional off diagonal terms which couple the order parameters of the two dimensional representation with d-wave symmetry and another term which mixes the d-wave and s-wave order parameters. Since the presence of these off diagonal coupling terms will enhance the upper critical field in general, the $(1,0,0)$ field direction will have a higher H_{c2} than the H_{c2} along $(1,1,0)$. The role of s-d mixing in comparing the H_{c2} for the (1,1,1) and the (1,1,0) magnetic field direction requires a more detailed approach. For $|T - T_c| << T_s - T_d$, we can use a perturbation theory which treats the Hamiltonian corresponding to the s-d mixing as a perturbation (with the s-wave state is the ground state). Defining the second order correction ($E^{(2)}$) to the s-wave eigenvalue as

$$\frac{|\alpha_s|}{\kappa_1} = \frac{1}{l^2} + E^{(2)} \tag{24}$$

we have

$$E^{(2)} = \sum_m{}' \left(\frac{|<0|H'|\chi_{1m}>|^2}{E_0 - E_{1m}} + \frac{|<0|H'|\chi_{2m}>|^2}{E_0 - E_{2m}} \right) \tag{25}$$

$$H'_{110} = k_4/(2l^2)(1 + 2\Pi_+\Pi_- + 3(\Pi_+^2 + \Pi_-^2)) \tag{26}$$

$$H'_{111} = k_4/l^2(\Pi_+^2 + \Pi_-^2) \tag{27}$$

In the above expression for the perturbed Hamiltonian, the 2D representation of cubic symmetry has been expressed in the $\eta_1 = (1, \omega, \omega^2)$, $\eta_2 = \eta_1^*$ basis, where $\omega = e^{2\pi i/3}$. Also the states $|\chi_m>$ are the eigenstates of the unperturbed Hamiltonian derived from the diagonalization of the η_1,η_2 free energy. The solutions can be expressed in terms of Landau level wave function. For the field along the (1,1,0) direction the eigenstates are

$$\chi_{1m} = \phi_m(\epsilon_1 x, y/\epsilon_1) \tag{28}$$

$$\chi_{2m} = \phi_m(\epsilon_2 x, y/\epsilon_2) \tag{29}$$

$$\epsilon_1^2 = \sqrt{\frac{\kappa_1 - 2\kappa_2}{\kappa_1 + \kappa_2}} \tag{30}$$

$$\epsilon_2^2 = \sqrt{\frac{\kappa_1 + 2\kappa_2}{\kappa_1 - \kappa_2}} \tag{31}$$

where ϕ_m represent the m^{th} Landau level solution. Similarly for the field along the (1,1,1) direction the eigenstates χ_{1m}, χ_{2m} are of the form, $a_m|m> + b_m|m+2>$ where a_m and b_m are known functions. It is found upon solving this problem numerically that the second order correction to the energy will be given by,

$$E^{(2)}_{111} \approx -\frac{8(\kappa_4/\kappa_1)^2}{l^4(T_s - T_d)} \tag{32}$$

$$E^{(2)}_{110} \approx -\frac{9.5(\kappa_4/\kappa_1)^2}{l^4(T_s - T_d)} \tag{33}$$

therefore the (1,1,0) direction provides a higher upper critical field than the (1,1,1) magnetic field direction near T_c. The GL theory given above thus yields the same anisotropy as seen experimentally, *independent of the values of the coefficients* κ_i.

B. Anisotropic London theory

Now we turn to the hexagonal to square vortex lattice transition that occurs at low fields[25]. The free energy of Eq. 1 contains too many undetermined coefficients to carry this out. We therefore use the weak-coupling theory described above to find the coefficients in the GL free energy. Of particular relevance, we find that the coefficients β_2, β_5, k_4, and k_3 are relatively small and we neglect them in the following. The GL theory can then be used to construct a London theory valid at low fields. We take $\psi_i = \psi_0 e^{i\phi_i}$, where $|\psi_0|$ takes on the bulk uniform solution value. This yields the following London free energy density

$$\begin{aligned} f_L = f_0 &+ (\epsilon|\psi_0|^2 + \beta_4|\psi_0|^4)[\cos(\phi_1 - \phi_2) + \cos(\phi_2 - \phi_3) + \cos(\phi_3 - \phi_1) - 3] \\ &+ \kappa_1|\psi_0|^2 \sum_i (\nabla_i \phi_i - 2eA_i)^2 + \kappa_2|\psi_0|^2 \sum_i (\nabla \phi_i - 2e\boldsymbol{A})^2 \end{aligned} \tag{34}$$

where f_0 is the free energy in the homogeneous state. Let us define $\phi_1 = \theta + \eta_1 - \eta_2/\sqrt{3}$, $\phi_2 = \theta - \eta_1 - \eta_2/\sqrt{3}$, and $\phi_3 = \theta + 2\eta_2/\sqrt{3}$. We expand f_L to quadratic order in η_1 and η_2 (this is valid when $\kappa_1/\epsilon << a^2$, where a is the spacing between vortices). We then solve for θ, η_1 and η_2 to find the following non-local London free energy

$$f_L = \frac{1}{8\pi}[\boldsymbol{B}^2 + \lambda_0^2(\nabla \times \boldsymbol{B})^2 + \frac{4\kappa_1}{3|\epsilon|\lambda_0^2}\frac{\kappa_1}{3\kappa_2 + \kappa_1}(\partial_x \partial_y B_z)^2] \tag{35}$$

where λ_0 is the penetration depth. Eq. 35 has the same form as the non-local London theory used by Kogan[28] to examine the hexagonal to square transition. The important point here is that the non-local correction (the third term in Eq. 35) is due to appearance of d-wave order and it is possible for this term to become large at relatively low fields, when $\kappa_1/\epsilon \approx a^2 \approx B/\Phi_0$ (Φ_0 is the superconducting flux quantum). This would push the hexagonal to square transition to low fields, in agreement with experiment. However when $\kappa_1/\epsilon > a^2$, the non-local London theory no longer applies. To understand the physics in this regime requires numerical analysis. Some understanding can be found by setting $\epsilon = 0$ and $\beta_4|\psi_0|^2 = 0$. In this case, the three order parameters ψ_i become decoupled and the vortex cores for each component are smaller than that of the pure s-wave theory. This is consistent with the observed shrinking of the vortex core[26,27]. While more analysis is required, the above shows that the low field hexagonal to square transition and shrinking of the vortex cores is consistent with the appearance of a d-wave component in magnetic fields.

VI. CONCLUSION

In conclusion we have argued that in $A15$ superconductors an attractive d-wave pairing channel exists in addition to the s-wave pairing channel. Using a microscopic weak coupling analysis we derive a Ginzburg Landau free energy for this system. The strength of this model lies in its ability to explain a number of relatively recent experimental observation within this single picture. It is shown that this d-wave pairing channel accounts for the sharp Raman resonance seen in the s-wave superconducting state. Furthermore, this d-wave pairing is induced by magnetic fields and can account for the observed anisotropy in the upper critical field and the observation of a sharp reduction of the superconducting coherence length at a hexagonal to square vortex lattice transition that appears at anomalously low fields.

ACKNOWLEDGMENTS

This work was supported by NSF grant DMR-0906633. We thank Steve Kivelson, Sonny Rhim, Manfred Sigrist, Kazuo Ueda, and Michael Weinert for useful discussions.

[1] J.P. Davis et al. Nature Physics **4**, 571 (2008).
[2] M. Fogelström, D. Rainer, J. A. Sauls, Phys. Rev. Lett. **79**, 281 (1997).
[3] K. Kuroki et al. Phys. Rev. Lett. **101**, 087004 (2008).
[4] W. C. Lee, S. C. Zhang, and C. Wu, Phys. Rev. Lett. **102**, 217002 (2009).
[5] R. Hackl and R. Kaiser, J. Phys. C: Solid State Phys. **21**, L453 (1988).
[6] B. T. Matthias et al. Phys. Rev. **95**, 1435 (1954).
[7] S. A. Geller, Acta Cryst. **9**, 885 (1956).
[8] B. W. Batterman, Phys. Rev. Lett. **13**, 390 (1964).
[9] G. Shirane, Phys. Rev. B **4**, 2957 (1971).
[10] J. Labbe and J. Friedel, J. Phys. Radium **27**, 153 (1966).
[11] L. P. Gorkov, Sov. Phys. JETP **9**, 1364 (1959).
[12] L. F. Mattheiss, Phys. Rev. B **12**, 2161 (1975).
[13] T. W. Mihalisin and R. D. Parks, in Low Temperature Physics, LT9, edited by J. B. Daunt, D. O. Edwards, F. J. Milford, and M. Yaqub (Plenum, New York, 1965).
[14] T. Jarlborg, A. A. Manuel, and M. Peter, Phys. rev. B **27**, 4210 (1983).
[15] A. J. Leggett, Prog. Theor. Phys. **36**, 901 (1966).
[16] P. Kumar and P. Wolfle, Phys. Rev. Lett. **59**, 1954 (1987).
[17] L. F. Mattheiss and W. Weber, Phys. Rev. B **25**, 2248 (1982).
[18] R. N. Bhatt, Phys. Rev. B **16**, 1915 (1977).
[19] L. Pintschovius, H. Takei, and N. Toyota, Phys. Rev. Lett. **54**, 1260 (1985).
[20] J. Geerk, U. Kaufmann, W. Bangert, and H. Rietschel, Phys. Rev. B **33**, 1621 (1986).
[21] T. Jarlborg, A. A. Manuel, and M. Peter, Phys. rev. B **27**, 4210 (1983).
[22] P. Morel, and P. W. Anderson, Phys. Rev. **125**, 1263 (1962).
[23] V. P. Mineev and K. V. Samokhin, Introduction to Unconventional Superconductivity (Gordon and Breach, London, 1999).
[24] M. N. Khlopkin, JETP Letters **69**, 26 (1999).
[25] Yethiraj, M., Christen, D.K., McK.Paul, D., Miranovic, P., Thompson, J.R., Phys. Rev. Lett. **82**, 5112 (1999).
[26] R. Kadono et al. Phys. Rev. B **74**, 024513 (2006).
[27] J. E. Sonier et al. Phys. Rev. Lett. **93**, 017002 (2004).
[28] Kogan, V.G., Miranovic, P., Dobrosavljevic-Grujic, L., Pickett, W.E., Christen, D.K., Phys. Rev. Lett. **79**, 741 (1997).